NASA TECHNICAL NOTE

NASA TN D-2077

NASA TN D-2077
C.1

HEAT TRANSFER FROM FIN-TUBE RADIATORS INCLUDING LONGITUDINAL HEAT CONDUCTION AND RADIANT INTERCHANGE BETWEEN LONGITUDINALLY NONISOTHERMAL FINITE SURFACES

by E. M. Sparrow, V. K. Jonsson, and W. J. Minkowycz

University of Minnesota
Minneapolis, Minnesota

NATIONAL AERONAUTICS AND SPACE ADMINISTRATION • WASHINGTON, D. C. • DECEMBER 1963

TECHNICAL NOTE D-2077

HEAT TRANSFER FROM FIN-TUBE RADIATORS INCLUDING LONGITUDINAL HEAT CONDUCTION AND RADIANT INTERCHANGE BETWEEN LONGITUDINALLY NONISOTHERMAL FINITE SURFACES

By E. M. Sparrow, V. K. Jonsson, and W. J. Minkowycz

University of Minnesota
Minneapolis, Minnesota

NATIONAL AERONAUTICS AND SPACE ADMINISTRATION

HEAT TRANSFER FROM FIN-TUBE RADIATORS INCLUDING LONGITUDINAL HEAT CONDUCTION AND RADIANT INTERCHANGE BETWEEN LONGITUDINALLY NONISOTHERMAL FINITE SURFACES

By E. M. Sparrow, V. K. Jonsson, and W. J. Minkowycz

SUMMARY

Consideration is given herein to two effects that have generally been neglected in prior studies of fin-tube radiators: (1) the longitudinal conduction of heat in the fin and (2) the effect of longitudinal temperature variation and finite radiator length on the radiant interchange between radiator elements. It is shown that longitudinal conduction is negligible for practical values of the governing parameters appropriate to space-vehicle power systems. It is also demonstrated that the radiant interchange can be calculated with sufficient accuracy by assuming longitudinally isothermal surfaces that are essentially infinite in length. These conclusions indicate that the problem can be treated in a quasi-two-dimensional manner. Results based on a quasi-two-dimensional model can be generalized to the case of a longitudinally varying temperature by a step-by-step method described herein.

INTRODUCTION

The need to dissipate energy from vehicles operating in atmosphere-free space has stimulated considerable interest in the characteristics of finned surfaces that transfer heat by thermal radiation. Consideration has been extended to thin plate-type fins, one edge of which is joined to a tube containing a flowing fluid from which heat is to be extracted. Figure 1 illustrates one of several radiator configurations utilizing such fins.

The initial analyses of radiating fins were concerned with a single isolated fin that radiates freely to space and which in turn may be irradiated from space; references 1 and 2 are representative of such literature. Later analytical treatments have considered the effects of radiant interaction between the fin and the tube or between neighboring fins of an ensemble that are able to view each other (e.g., refs. 3 and 4).

In formulating the energy balances from which heat-transfer solutions for plane fins are ultimately derived, it has been standard to concentrate on the transport processes that take place in the plane of a typical cross section of the fin. Heat conduction normal to the plane of the fin cross section is

neglected. Additionally, as far as radiant transport is concerned, it is tacitly assumed that temperature variations in the direction normal to the cross section are negligible[1] and that the length of the fin in this direction is effectively infinite. As a consequence of these assumptions, the radiating-fin problem is reduced essentially to a plane problem.

There are situations in which temperature variations normal to the fin cross section necessarily occur, for example, when a single-phase fluid such as a liquid metal or a gas flows through the tube. For such situations, it has been proposed to apply the aforementioned solutions locally in a step-by-step manner along the length of the radiator (i.e., along the direction of the fluid flow). Such a calculation procedure neglects the effects of the longitudinal temperature variation on the heat conduction and on the radiant interaction between the fin and tube surfaces, if such interaction exists.

It is the purpose of this report to reexamine the three-dimensional effects in a quantitative manner and to evaluate the validity of the currently standard plane formulation. The investigation to be described is divided into two parts. The first part deals with the effects of heat conduction normal to the plane of the fin cross section. The second part is concerned with the effects of a longitudinal temperature gradient and of finite radiator length on the radiant interaction between fin and tube surfaces.

This research was sponsored by the National Aeronautics and Space Administration through the Office of Grants and Research Contracts.

SYMBOLS

A surface area

c_p constant-pressure specific heat of fluid

e_i energy incident on fin surface element per unit time and area

F angle factor

h fin half-width

k thermal conductivity of fin material

L radiator length

$\dot{m}$ fluid flow rate

N_b base-surface temperature parameter, $4ktL/\dot{m}c_p h$

N_c fin-conductance parameter, $\epsilon\sigma T_b^3 h^2/kt$

[1]This situation is approximated when there is a two-phase flow through the tubes with small pressure drops.

N_{ci}	fin-conductance parameter based on T_{bi}
R	tube radius
T	absolute temperature
T^*	equivalent temperature of surrounding space
T_b	temperature of fin base
T_{bi}	base temperature at $z = 0$
t	fin half-thickness
X	dimensionless coordinate, x/h
x	coordinate measuring distance across fin width
y	coordinate measuring distance across fin thickness
Z	dimensionless coordinate, z/L
z	coordinate measuring distance along fin or tube length
ϵ	fin surface emittance
η	conventional fin effectiveness
Θ	dimensionless temperature, T/T_{bi}
Θ^*	dimensionless equivalent space temperature, T^*/T_{bi}
Θ_b	dimensionless fin-base temperature, T_b/T_{bi}
θ	dimensionless temperature, T/T_b
θ^*	dimensionless equivalent space temperature, T^*/T_b
σ	Stefan-Boltzmann constant

Subscripts:

bL	base at $z = L$
f	fin
t	tube
0,1,2,3,4	mesh points, fig. 2
1,2	tubes 1 and 2, fig. 3

ANALYTICAL FORMULATION FOR LONGITUDINAL CONDUCTION

Consideration is given to the plate-type radiating fin that is pictured schematically in figure 2. The fin thickness is $2t$, the width is $2h$, and the length is L. The edges of the fin at $x = 0$ and $x = 2h$ are attached to tubes through which a fluid is flowing. Except in a two-phase flow with negligible pressure drop, the fluid temperature will change during the course of its passage through the tube. Correspondingly, the temperature T_b at the fin base may be a function of the longitudinal coordinate z. It is assumed that identical thermal conditions exist along $x = 0$ and $x = 2h$. Consequently, the line $x = h$ is a symmetry line.

In the currently standard formulation of the radiating-fin problem, the heat conduction in the z-direction is neglected. Furthermore, within the framework of thin-fin theory, the temperature is essentially independent of y. Therefore, the energy conservation principle reduces to a balance between heat conduction in the x-direction and thermal radiation at the surface. For negligible radiant interaction between fin and tube, the form of the heat-balance equation that has become conventional in the study of radiating fins is

$$2kt \frac{d^2T}{dx^2} = 2\sigma\epsilon(T^4 - T^{*4}) \tag{1}$$

where T^* is the equivalent temperature of the radiation from space that is incident upon the fin. The factor of 2 that appears on the right side of equation (1) implies a symmetrical radiation to and from both sides of the fin.

Equation (1) is made dimensionless by defining

$$\left.\begin{aligned} X &= x/h & \theta &= T/T_b \\ N_c &= \epsilon\sigma T_b^3 h^2/kt & \theta^* &= T^*/T_b \end{aligned}\right\} \tag{2}$$

from which it follows that

$$\frac{d^2\theta}{dX^2} = N_c(\theta^4 - \theta^{*4}) \tag{3}$$

The boundary conditions appropriate to the temperature variable θ are $\theta = 1$ at $X = 0$ and $d\theta/dX = 0$ at $X = 1$. Solutions of equation (3) depend parametrically on prescribed values of N_c and θ^*.

Within the framework of this formulation, the possible dependence of T_b on the longitudinal coordinate z does not appear directly, although both N_c and θ^* are functions of z if T_b depends on z. The only role of this dependence would be perhaps to influence the selection of numerical values for the parameters N_c and θ^*.

Conduction of heat in the z-direction may be included in the analysis by adding $2kt(\partial^2T/\partial z^2)$ to the left side of equation (1), which gives

$$2kt\left(\frac{\partial^2 T}{\partial x^2}+\frac{\partial^2 T}{\partial z^2}\right)=2\sigma\epsilon(T^4-T^{*4}) \tag{4}$$

The inclusion of the temperature variation in the z-direction requires that suitable boundary conditions be specified. The symmetry condition that $\partial T/\partial x = 0$ at $x = h$ continues to apply, but the fin-base temperature T_b depends on z. It is also necessary to stipulate the thermal conditions along the edges $z = 0$ and $z = L$. In practice, these conditions depend on the detailed configuration of the radiator. With a view toward keeping the analysis general, the adiabatic boundary condition $\partial T/\partial z = 0$ is imposed along these edges. Based on experience with convective fins, it is expected that the use of such a boundary condition will have a negligible effect on the final heat-transfer results when the fin is thin.

An explicit specification of $T_b(z)$ is needed. In general, for fluid flowing through a tube attached to the edge at $x = 0$, the local value of T_b could be related to the local bulk temperature of the fluid by means of a heat-transfer coefficient and a conductive resistance. In turn, the local bulk temperature would be determined from an energy balance on the fluid. In view of the purposes of the present investigation, however, a somewhat simpler procedure is to be employed. It is the aim of this study to provide insight into the effects of longitudinal conduction by comparing the results calculated from equation (4) with those calculated by a step-by-step application of the solutions of equation (3). The essential matter is the comparison between the two sets of results, the absolute numerical values being of lesser consequence. From this point of view, the analysis is simplified by taking the local fluid temperature and the local fin-base temperature to be the same. In general, it is expected that this approximation would exaggerate the longitudinal temperature gradient along the fin base. For flows with high heat-transfer coefficients (e.g., liquid metals or internally finned gas flows), however, the foregoing assumption is very nearly satisfied. With this, an energy balance on the fluid yields

$$\dot{m}c_p\,dT_b = 2\left[2kt\,dz(\partial T/\partial x)_{x=0}\right] \tag{5}$$

in which the left side is the change of enthalpy of the flowing fluid and the right side is the heat conducted into a pair of fins attached to the tube. For simplicity, the direct radiant-heat loss from the tube surface to space is not included in this energy balance inasmuch as it is not essential for the purposes of the present investigation.[2]

In forming a dimensionless temperature variable, it is convenient to employ as a standard the entering fluid temperature, which within the present approximation is equal to T_b at $z = 0$. This is denoted by T_{bi}. If one additionally defines

---

[2]The effect of the radiant-heat loss from the tube would be to alter the temperature change of the flowing fluid. For the purpose of this analysis, however, any desired change in fluid temperature can be achieved by suitable selection of the forthcoming N_b parameter.

$$\left.\begin{aligned} X &= \frac{x}{h} \qquad \Theta = \frac{T}{T_{bi}} \\ Z &= \frac{z}{L} \qquad \Theta^* = \frac{T^*}{T_{bi}} \\ & \qquad \Theta_b = \frac{T_b}{T_{bi}} \end{aligned}\right\} \tag{6a}$$

$$N_{ci} = \frac{\epsilon\sigma T_{bi}^3 h^2}{kt} \qquad N_b = \frac{4ktL}{\dot{m}c_p h} \tag{6b}$$

equations (4) and (5) become

$$\frac{\partial^2\Theta}{\partial X^2} + \left(\frac{h}{L}\right)^2 \frac{\partial^2\Theta}{\partial Z^2} = N_{ci}\left[\Theta^4 - \Theta^{*4}\right] \tag{7a}$$

$$d\Theta_b = N_b(\partial\Theta/\partial X)_{X=0}\, dZ \tag{7b}$$

The boundary conditions can also be represented in dimensionless form as

$$\left.\begin{aligned} \partial\Theta/\partial X &= 0 \quad \text{at} \quad X = 1 \\ \partial\Theta/\partial Z &= 0 \quad \text{at} \quad Z = 0 \quad \text{and} \quad Z = 1 \end{aligned}\right\} \tag{8}$$

Inspection of the foregoing equations reveals that two new parameters, h/L and N_b, have been added to the problem in addition to N_{ci} and Θ^*.

Solutions

A closed-form analytical solution of the mathematical system represented by equations (7) and (8) cannot be achieved. Fortunately, solutions may be carried out by numerical means. To accomplish such solutions, a finite-difference representation of the governing equations is needed. With the aid of the finite-difference mesh indicated in figure 2, one can write

$$\partial^2\Theta/\partial X^2 = \left[\Theta_1 + \Theta_3 - 2\Theta_0\right]/\Delta X^2 \tag{9a}$$

$$\partial^2\Theta/\partial Z^2 = \left[\Theta_2 + \Theta_4 - 2\Theta_0\right]/\Delta Z^2 \tag{9b}$$

In addition, the Θ^4 appearing in equation (7a) corresponds to Θ_0^4.

There are actually a variety of forms into which the finite-difference representation of the energy conservation equation can be cast, and it is desirable to investigate which is most advantageous for the calculation. To check this

matter, one may return to the simpler equation (3), for which highly accurate numerical solutions have been carried out by other techniques. Several finite-difference forms of equation (3) can be constructed, four of which are

$$\theta_0 = \frac{1}{2}(\theta_1 + \theta_3) - \frac{1}{2} N_c \Delta X^2 \theta_0^4 \tag{10a}$$

$$\theta_0 = \left[(\theta_1 + \theta_3 - 2\theta_0)/N_c \Delta X^2\right]^{1/4} \tag{10b}$$

$$\theta_0 = (\theta_1 + \theta_3)/(2 + N_c \Delta X^2 \theta_0^3) \tag{10c}$$

$$\theta_0 = \left\{(\theta_1 + \theta_3)\Big/\left[(2/\theta_0) + N_c \Delta X^2 \theta_0^2\right]\right\}^{1/2} \tag{10d}$$

The θ^* term has been omitted for simplicity.

Any of the foregoing may be utilized in an iterative calculation scheme that may be executed on a digital computer. One begins by guessing the θ values at all the mesh points on the line from $X = 0$ to $X = 1$. With this, the numerical values of θ_0, θ_1, and θ_3 that appear on the right side of the finite-difference equations are available. The θ_0 appearing on the left side can then be calculated. In this way, new θ values for all mesh points can be obtained and the procedure continued until convergence is achieved.

Equations (10a) to (10d) were programmed for the Univac 1103 computer, and iterative solutions attempted with each. Equation (10c) led to smooth convergence of the iterative procedure, while difficulties were encountered with the others. Furthermore, a mesh size $\Delta X = 0.1$ led to a converged result that was in very close agreement with prior numerical solutions performed by other methods.

A finite-difference form of equation (7a), which is an appropriate generalization of equation (10c), is

$$\Theta_0 = \frac{\Theta_1 + \Theta_3 + \left(\frac{h}{L}\right)^2\left(\frac{\Delta X}{\Delta Z}\right)^2(\Theta_2 + \Theta_4)}{2\left[1 + \left(\frac{h}{L}\right)^2\left(\frac{\Delta X}{\Delta Z}\right)^2\right] + N_c \Delta X^2 \Theta_0^3} \tag{11}$$

in which Θ^* has been taken to be zero to reduce the number of parameters. In addition, the condition (7b) for determining $\Theta_b(Z)$ takes the form

$$\Theta_b(Z + \Delta Z) = \Theta_b(Z) + N_b \left(\frac{\partial\Theta}{\partial X}\right)_{X=0} \Delta Z \tag{12a}$$

in which

$$\left(\frac{\partial\Theta}{\partial X}\right)_{X=0} = \frac{1}{2}\left[\frac{\partial\Theta}{\partial X}(0,Z) + \frac{\partial\Theta}{\partial X}(0,Z + \Delta Z)\right] \tag{12b}$$

The derivatives in the brackets were evaluated numerically by applying a standard five-point right-hand difference formula

$$\frac{\partial\Theta}{\partial X}(0,Z) = \frac{1}{12\,\Delta X}\left[-25\Theta_b(Z) + 48\Theta(\Delta X,Z) - 36\Theta(2\Delta X,Z) + 16\Theta(3\Delta X,Z) - 3\Theta(4\Delta X,Z)\right] \tag{12c}$$

From the foregoing, it is clear that the boundary condition along $X = 0$, that is, the $\Theta_b(Z)$, does not remain fixed during an iterative computation, but rather changes from one cycle of the iteration to the next. This is one of the interesting and novel computational features of the present problem. Finally, the adiabatic conditions of equation (8) were accounted for by making standard modifications in equation (11) at the boundary points.

The solution for the temperature can, in principle, be carried out by applying equations (11) and (12) in an iterative manner. One may begin by guessing the temperatures at all the mesh points in the grid. With these, new values of Θ may be calculated by successive application of equation (11) at all points except those along the line $X = 0$. The latter are found by application of equation (12a) once the derivatives $\overline{(d\Theta/dX)}_{X=0}$ have been computed from equations (12b) and (12c). In this way, new values of Θ are made available at all points of the grid and the next cycle of the iteration may be begun.

In practice, it is readily found that such an iterative procedure does not converge; in fact, the Θ values diverge after a few cycles of the iteration. To understand and to surmount this difficulty, it is necessary to consider the computation process in greater detail. In connection with the difference formula (12c), it may be noted that, if the values of $\Theta_b(Z)$, $\Theta(\Delta X,Z)$, $\Theta(2\Delta X,Z)$, and so forth, are not smooth, the derivative calculated from equation (12c) is in error and so is Θ_b. Such errors serve as sources of instability and ultimately cause divergence of the iterative procedure.

Further consideration suggests that the $\Theta_b(Z)$, $\Theta(\Delta X,Z)$, $\Theta(2\Delta X,Z)$, and so forth, are not smooth if $\Theta_b(Z)$ is recalculated at each cycle of the iterative process, particularly during the early cycles of the calculation when all values of Θ are approximate. For this reason, the iterative procedure was modified so that $\Theta_b(Z)$ is reevaluated only once in every n cycles of the iteration - the number n being equal to the number of mesh points lying in the x-direction between $0 < X \leq 1$. In other words, n cycles of the iteration are carried out with fixed $\Theta_b(Z)$, then $\Theta_b(Z)$ is reevaluated, n additional cycles are carried out, and so forth. This procedure permits the effect of a change in Θ_b to be felt at all points in the mesh before the next change in Θ_b is made. In the present calculations, n was equal to 10. In the later stages of the iterative process, when convergence is being approached, $\Theta_b(Z)$ can be recalculated once every 5 cycles without giving rise to instability.

Results

Consideration of proposed radiator configurations for space-vehicle power systems suggests that it is quite unlikely that the aspect ratio h/L will

exceed 1/30. Additionally, it was found by calculation that a realistic value of N_{ci} for such applications is 1. Corresponding to these values of h/L and N_{ci}, solutions to equation (11) were carried out for $N_b = 0.7$ and $N_b = 0.4$.

From among the totality of Θ values determined from these solutions, the $\Theta_b(Z)$ are perhaps of greatest interest because they correspond most closely to the distribution of the fluid temperature. In particular, Θ_b at $Z = 1$ corresponds to the ratio of the fluid temperature at the outlet to the fluid temperature at the inlet. Therefore, $\Theta_b(1)$ is an indication of the heat loss from the fin. The $\Theta_b(Z)$ from the solutions of equation (11) are listed in table I for $N_b = 0.7$ and $N_b = 0.4$. To illustrate the fluid temperature changes embodied in these solutions, it is seen from table I(b) that for $N_b = 0.7$ there will be a temperature change between the inlet and the outlet of 400° F if $T_{bi} = 1600^\circ$ R.

The temperature results determined from equation (11) are now compared with an alternative set of results based on a step-by-step application of the solutions of equation (3). The underlying assumption of this step-by-step calculation is that longitudinal conduction can be neglected. On this basis, the length of the fin L is divided into a set of strips, each having a width Δz. To each such strip, a conductive-radiative energy balance having the form of equation (3) is applied. Because the fin-base temperature $T_b(z)$ at z would not be known a priori, however, neither would the corresponding value of N_c that appears in equation (3). The local values of T_b and N_c can be found by the procedure described in the following paragraphs.

The first task in the procedure is to solve equation (3) for a succession of N_c values that span the range of interest. These solutions were carried out by utilizing the finite-difference equation (10c). The derivatives $\left[d(T/T_b)/dX\right]_{X=0}$ that were thus obtained are listed in table II as a function of N_c. It may be noted that this derivative is related to the conventional fin effectiveness η as follows:

$$\left[d(T/T_b)/dX\right]_{X=0} = -\eta N_c$$

The basic calculation formulas for the step-by-step method are equations (12a) and (12b). The essential feature of the calculation is that the derivatives appearing on the right side of equation (12b) are evaluated from table II or a plot thereof. To begin the calculation, one has the given values $\Theta_b(0) = 1$ and N_{ci} at $Z = 0$. Corresponding to N_{ci}, the derivative $\left[d(T/T_b)/dX\right]_{X=0}$ is available from table II. Then, a guess is made of Θ_b at the first point $Z = \Delta Z$. With this guess N_c at $Z = \Delta Z$ can be calculated as follows:

$$N_c(\Delta Z) = N_{ci}\left[\Theta_b(\Delta Z)\right]^3$$

and the corresponding $\left[d(T/T_b)/dX\right]_{X=0}$ may be read from table II. The $d\Theta/dX$ needed in equation (12b) is evaluated from the identity

$$\frac{d\Theta}{dX} = \left(\frac{T_b}{T_{bi}}\right) \frac{d(T/T_b)}{dX} = \Theta_b \frac{d(T/T_b)}{dX}$$

With this information, the derivative $\overline{(d\Theta/dX)}_{X=0}$ can be computed from equation (12b), and a value of Θ_b at $Z = \Delta Z$ may be found from (12a). If this new value of Θ_b at $Z = \Delta Z$ coincides with the previously guessed value, the first step has been taken successfully. If not, one makes a new guess and repeats the procedure.

Utilizing the aforementioned procedure, one may proceed in a step-by-step manner along the fin base from $Z = 0$ to $Z = 1$. The results of such a stepwise calculation are listed in table I in an arrangement convenient for comparison with the results calculated from equation (11), the latter including longitudinal conduction. An inspection of the two sets of results reveals differences that are no greater than 1 in the fourth decimal place. Such differences are fully negligible. Thus, on the basis of the foregoing comparison, it appears that longitudinal conduction in the fin is completely negligible for the parameter values chosen in this investigation. It is not believed that the substance of this conclusion is affected by the simplifying assumptions of the foregoing analysis. The parameter values for which numerical results were reported were chosen for liquid-cycle systems. For gas cycles, however, the N_b parameter might well exceed 0.7, which was the largest value included in this study. The effect of a larger N_b value would be to increase the temperature drop of the flowing fluid. On the other hand, the h/L parameter for the gas-cycle radiator is likely to be smaller than the value of 1/30 employed in the calculations. By inspection of equation (7), it is seen that a decrease in h/L, for example, from 1/30 to 1/60, tends to reduce the effect of longitudinal conduction by a factor of 4. Therefore, the larger longitudinal temperature differences that might be encountered in a gas-cycle system would not change the substance of the conclusion stated in the foregoing.

LONGITUDINAL RADIANT TRANSPORT

In order for there to be radiant interchange between radiator elements, it is necessary that there be a direct view between such elements. There is a wide variety of radiator configurations in which radiant interaction can occur. For concreteness, consideration is given herein to the fin-tube arrangement of figure 1. A more detailed representation of this configuration is shown in figure 3 to facilitate discussion of the radiant-interchange problem.

There are two types of radiant interaction that may occur in such a configuration. First, radiant energy from the tube surfaces may be incident upon the fin. Second, radiant energy from the fin may be incident upon the tubes. In general, such interchange includes radiation that is both emitted and reflected from the participating surfaces. To simplify the present discussion, the fin and tube surfaces are taken to be essentially black so that interreflected radiation may be neglected. In addition, it is assumed that the temperature of each tube is circumferentially uniform and varies only along the length and that both tubes have the same temperature.

The radiant interaction problem connected with the fin-tube arrangement of figure 3 is considered in reference 4, but in a quasi-two-dimensional manner. It is assumed in that analysis that the radiation arriving at an elemental area of fin comes from a pair of tube surfaces that are both circumferentially and longitudinally isothermal and of infinite length. Also, the radiation arriving at an element of tube surface is assumed to come from a longitudinally isothermal fin of infinite length. The dual assumptions of longitudinal isothermality and infinite length permit the longitudinal transport of radiation to be accounted for in a very simple manner which, in effect, removes the third (longitudinal) dimension from the problem. In fact, in the final formulation, the problem has the appearance of being two-dimensional (in the cross section of the fin and tubes).

When consideration is given to longitudinal temperature variations and to finite-length surfaces, the radiant interaction does not appear, at first glance, to lend itself to treatment by the simple methods of reference 4. To solve the fin-tube radiator completely, including such nonelementary radiant interactions is an exceedingly lengthy computational task, although there are no conceptual difficulties in the analysis. Clearly, the quasi-two-dimensional treatment of reference 4 would be preferable provided that it could be applied without significant loss of accuracy. It is the present purpose to explore the adequacy of the quasi-two-dimensional treatment of the radiant interchange. In the forthcoming analysis, longitudinal conduction is neglected in accordance with the earlier findings of this report.

Effect on Fin Heat Transfer

Consideration is first given to the effects of the radiant interaction on the heat loss from the fin. The energy balance for an elementary volume of fin may be found by generalizing equation (1) to include radiant energy incident upon the fin from the tube surfaces. From an element of tube surface, such as dA_1 (fig. 3), there is emitted in all directions an energy quantity $\sigma\left[T_b(z_t)\right]^4 dA_1$. Of this, an amount $\sigma(dA_1/dA_f)\left[T_b(z_t)\right]^4 dF_{dA_1-dA_f}$ arrives per unit area at an elementary fin area dA_f. The symbol $dF_{dA_1-dA_f}$ denotes the angle factor for diffuse interchange between dA_1 and dA_f. According to the reciprocity relation for diffuse angle factors, $dA_1\, dF_{dA_1-dA_f} = dA_f\, dF_{dA_f-dA_1}$. With this, the energy arriving at dA_f from dA_1 can be written as $\sigma\left[T_b(z_t)\right]^4 dF_{dA_f-dA_1}$; but dA_f receives radiant energy from all elements dA_1 on tube 1 as well as from all elements dA_2 on tube 2, and the total of such contributions is

$$e_i = \sigma \int_{z_t=0}^{L} \left[T_b(z_t)\right]^4 \left[dF_{dA_f-dA_1} + dF_{dA_f-dA_2}\right] \tag{13}$$

This incident energy quantity may be appended to equation (1), which may be specialized to the blackbody case by setting $\epsilon = 1$. In addition, as a simplification, T^* is taken to be zero. With these the energy balance becomes

$$kt \frac{d^2T}{dx^2} = \sigma T^4 - \sigma \int_0^L \left[T_b(z_t)\right]^4 \left[dF_{dA_f\text{-}dA_1} + dF_{dA_f\text{-}dA_2}\right] \tag{14}$$

The integral on the right side of equation (14) is an exact representation of the radiation emitted by the tubes that falls on the surface element dA_f located at position x,z on the fin. If the major part of this incident radiation were to originate at tube locations just opposite the fin surface element dA_f, that is, at locations $z_t \approx z$, one might propose to approximate the integral such that

$$e_i = \sigma\left[T_b(z)\right]^4 \int_{-\infty}^{\infty} \left[dF_{dA_f\text{-}dA_1} + dF_{dA_f\text{-}dA_2}\right] \tag{15}$$

Furthermore, according to reference 4, $\int_{-\infty}^{\infty} \left[dF_{dA_f\text{-}dA_1} + dF_{dA_f\text{-}dA_2}\right]$ may be carried out in closed form and is expressed by

$$\int_{-\infty}^{\infty} \left[dF_{dA_f\text{-}dA_1} + dF_{dA_f\text{-}dA_2}\right] \equiv F_{f\text{-}t} = 1 - \frac{1}{2}\left\{\frac{\sqrt{\left[(R/h) + X\right]^2 - (R/h)^2}}{(R/h) + X} + \frac{\sqrt{\left[(R/h) + 2 - X\right]^2 - (R/h)^2}}{(R/h) + 2 - X}\right\} \tag{16}$$

With this, an approximate form of the energy balance, equation (14), can be written for fin location z

$$kt \frac{d^2T}{dx^2} = \sigma T^4 - \sigma(F_{f\text{-}t})T_b^4(z) \tag{17}$$

in which $T_b^4(z)$ is a constant as far as the integration in x is concerned. Therefore, equation (17) can be solved without recourse to the longitudinal variation of the temperature, and the problem has a quasi-two-dimensional appearance.

It remains to ascertain whether the fin heat-transfer results calculated from the approximate equation (17) are an adequate representation of the heat-transfer results that would be calculated from equation (14). In proceeding with

this determination, it is reasonable to confine consideration only to those situations where the radiant interaction plays a nonnegligible role in the fin heat-transfer process. In reference 4 it is shown that for tube radii R up to $0.2\ h$, the radiant interaction affects the fin heat transfer by 7 percent or less when $N_c = 1$. Therefore, approximations in the calculation of the radiant interaction should have a minor effect on fin heat transfer for R/h values up to 0.2. On the other hand, it is not expected that practical radiator configurations would have R/h values exceeding 0.4. According to reference 4, the effect of the radiant interaction is to reduce the fin heat loss by 13 percent for $R/h = 0.4$ and $N_c = 1$. In light of the foregoing discussion, consideration is given to the case of $R/h = 0.4$.

In order to proceed with the analysis, it is necessary to know the angle factor

$$dF_{dA_f - dA_1} + dF_{dA_f - dA_2} = dF_{dA_f - (dA_1 + dA_2)}$$

where the representation on the right side is meant to indicate that the tube surface elements dA_1 and dA_2 are taken at the same z_t-coordinate. This angle factor may be derived by direct evaluation of the basic angle factor definition. When the indicated integrations are carried out, there results

$$\left[dF_{dA_f - (dA_1 + dA_2)}\right] \frac{2\pi(h/L)}{dZ} = \left\{ \frac{1}{2\tilde{X}} \ln \left[\frac{\left(\tilde{X} - \frac{R}{h}\right)^2 + \left(\frac{L}{h}\right)^2 Z^2}{\tilde{X}^2 - \left(\frac{R}{h}\right)^2 + \left(\frac{L}{h}\right)^2 Z^2} \right] - \frac{\frac{R}{h}\left(\frac{R}{h} - \tilde{X}\right)}{\tilde{X}\left[\left(\tilde{X} - \frac{R}{h}\right)^2 + \left(\frac{L}{h}\right)^2 Z^2\right]} \right\}$$

$$+ \left\{ \frac{1}{2\left[2\left(1 - \frac{R}{h}\right) - \tilde{X}\right]} \ln \left[\frac{\left(2 - 3\frac{R}{h} - \tilde{X}\right)^2 + \left(\frac{L}{h}\right)^2 Z^2}{\left[2\left(1 - \frac{R}{h}\right) - \tilde{X}\right]^2 - \left(\frac{R}{h}\right)^2 + \left(\frac{L}{h}\right)^2 Z^2} \right] \right.$$

$$\left. - \frac{\frac{R}{h}\left(3\frac{R}{h} - 2 + \tilde{X}\right)}{\left[2\left(1 - \frac{R}{h}\right) - \tilde{X}\right]\left[\left(2 - 3\frac{R}{h} - \tilde{X}\right)^2 + \left(\frac{L}{h}\right)^2 Z^2\right]} \right\} \qquad (18a)$$

in which Z has the same definition as previously, while $\tilde{X}$ denotes a shifted x-coordinate as follows:

$$\tilde{X} = X + (R/h) \qquad (18b)$$

To provide a feeling for the variation of this angle factor as a function of the longitudinal separation between dA_f and the elements dA_1 and dA_2, a representative tabulation is presented. This information, corresponding to

$x/h = 0.35$, is presented in table III. The R/h and h/L parameters have values of 0.4 and 1/30, respectively. Inspection of the table reveals that the angle factor drops off rapidly as Z_t deviates from Z. This suggests that the bulk of the radiation arriving at dA_f comes from the elements dA_1 and dA_2 that are located directly opposite dA_f, that is, at $Z_t \approx Z$. This conclusion tends to support the assumptions made in deriving the approximate energy equation (17). An even sharper dropoff in the angle factor would be observed at locations characterized by smaller values of x/h. On the other hand, the dropoff would be slower at locations near $x/h = 1$, where the radiant energy transfers are relatively small.

Additional information may be gathered by comparing the exact approximate values of the energy e_i incident at dA_f represented by equations (13) and (15). For convenience in carrying out the integration in equation (13), the variation of T_b with z_t is taken to be linear, that is,

$$T_b = T_{bi} - (T_{bi} - T_{bL})(z_t/L) \tag{19a}$$

or

$$\Theta_b = 1 - (1 - \Theta_{bL})Z_t \tag{19b}$$

It is recognized that the actual variation of T_b with z_t is not linear; however, the essential conclusions drawn are not prejudiced by this assumption. With T_b from equation (19a) and the angle factor from (18a), e_i may be evaluated in closed form from equation (13). Alternatively, an approximate value of e_i may be calculated from equation (15) in conjunction with equation (18a).

The results thus obtained are presented in table IV as a function of position X across the fin. The tabulated quantity is the ratio $e_i(X)/e_i(0)$, which is the ratio of the energy incident at location X to that incident at $X = 0$. Information is provided at longitudinal positions near the fluid inlet end of the radiator ($Z = 0.06$), at the midregion ($Z = 0.5$), and near the outlet end ($Z = 0.94$).[3] The fin-tube dimension parameter R/h corresponding to these results is 0.4, the radiator aspect ratio h/L is 1/30, and the longitudinal temperature ratio $\Theta_{bL}(=T_{bL}/T_{bi})$ is 0.5.

When these results are appraised, cognizance should be taken of the fact that the values of $e_i(0)$ calculated from equations (13) and (15) are negligibly different. Therefore, a comparison of the $e_i(X)/e_i(0)$ ratios corresponding to equations (13) and (15) immediately provides a measure of the approximation introduced when the latter is applied. By inspection of the tabulations it is seen that there is very little difference in the incident radiation calculated from equations (13) and (15). The largest deviations occur at longitudinal positions near the inlet end of the radiator, that is, at small Z (table IV(a)). Even

[3]Values of $Z = 0$ and $Z = 1.0$ were not used because it is expected that heat transfer in these regions might be dominated by the specific configuration of headers or manifolds used to distribute the fluid to the radiator. Under these circumstances, the effects considered here would be overridden by the presence of the headers or manifolds.

these differences are quite small, however.

In appraising the effect of these slight differences in e_i upon the fin heat loss, it is useful to consider the quantity $E_i = \int_0^1 e_i \, dX$, which is the total incident radiation on a longitudinal strip of fin. At the position $Z = 0.06$ the value of E_i based on equation (15) is 1.3 percent higher than that calculated from equation (13). It is shown in reference 4, however, that E_i is of the order of 13 percent of the energy radiated from the fin surface when $R/h = 0.4$ and $N_c = 1$. Thus, for these conditions an uncertainty of 1.3 percent in E_i gives rise to an uncertainty of only about 0.2 percent in the fin heat loss. The level of uncertainty is even smaller at the other longitudinal positions.

It would appear from the foregoing that the radiation incident on the fin can be calculated as if the tube surfaces were isothermal and of infinite length. From the mathematical point of view, this means that one may employ the simplified energy equation (17) in place of equation (14). The former is solved in reference 4 for a range of values of N_c and R/h. These solutions may be applied to a radiator having varying T_b by utilizing a step-by-step method similar to that devised earlier in the section Solutions.

Effect on Tube Heat Transfer

Consideration is now given to the effect of radiant interchange on the radiant-heat loss from the tubes. In particular, it is desired to determine whether the radiant energy incident on a tube surface element can be calculated as if the system were longitudinally isothermal and of infinite length. To simplify the discussion, it is assumed that the fin and tube surfaces are black and that T^* is negligible.

When referring to figure 3, it is seen that radiant energy arriving at a typical element of tube, such as dA_2, comes from the fin and the opposite tube. Attention is given first to the radiation from the fin that arrives at an element of tube surface. As a consequence of the reciprocity relation

$$dA_f\left(dF_{dA_f-dA_2}\right) = dA_2\left(dF_{dA_2-dA_f}\right)$$

it follows that the angle factors used in calculating the radiation from fin to tube are, in essence, the same as those used in calculating the radiation from tube to fin. From this, it further follows that the conclusions previously arrived at for the tube-to-fin radiation carry over to the fin-to-tube radiation. Since, as shown previously, longitudinal temperature variations and finite system length need not be considered in calculating the tube-to-fin radiation, the same should hold for the fin-to-tube radiation. In other words, one may calculate the radiation arriving at an element of tube located at z_t by supposing that the fin is longitudinally isothermal and infinite and has a temperature distribution $T(x)$ corresponding to that at $z = z_t$.

Next, consideration may be given to the radiant energy arriving at an elemental area of one tube from the opposite tube. From an evaluation of equations (15) and (18) of reference 5, it is readily shown that, for the condition $R/h = 0.4$, the incident energy quantity is of the order of 5 percent of the energy emitted by the area element. Therefore, approximations in the calculation of the incident energy have a very small effect on the heat loss from the tube. Nevertheless, an analysis is presented to determine the error involved when a simplified method of calculating the tube-to-tube radiant transfer is used.

The radiant energy arriving per unit area at element dA_2 due to emission from the opposite tube is

$$\sigma \int_{z_{t,1}=0}^{L} \left[T_b(z_{t,1})\right]^4 \, dF_{dA_2-dA_1} \tag{20}$$

The angle factor $dF_{dA_2-dA_1}$ that appears in the integral was derived as described in reference 5. To provide a feeling for the variation of the angle factor as a function of longitudinal separation between the elements, table V is presented. The results listed therein correspond to $R/h = 0.4$ and $h/L = 1/30$. It is seen that the angle factor drops off quite rapidly with longitudinal separation. This suggests that an approximation to equation (20) be attempted in the form

$$\sigma\left[T_b(z_t)\right]^4 \int_{-\infty}^{\infty} dF_{dA_2-dA_1} \tag{21}$$

in which $T_b(z_t)$ is the tube temperature at $z_{t,2} = z_{t,1}$.

Equation (20) has been evaluated by utilizing as input the linearly varying tube temperature of equation (19), with $\Theta_{bL} = 0.5$. This result may be compared with an alternative value calculated from equation (21). For tube surface elements that are located in the range $0.1 \leq Z_t \leq 0.9$, the incident energy calculated from equation (21) differs by about 0.5 percent from that calculated from equation (20). It may be recalled that the incident energy is itself only 5 percent of the emitted energy. Therefore, the uncertainty of 0.5 percent in the incident energy gives rise to an uncertainty of less than 0.05 percent in the heat loss. This uncertainty is, of course, fully negligible.

The use of equation (21) in place of equation (20) grows less exact near the inlet and outlet regions of the radiator, that is, for Z values near 0 and 1. The close proximity of headers and manifolds to these regions suggests, however, that other effects may well outweigh the approximation made in the calculation of the tube-to-tube radiant interchange.

From the foregoing discussion, it would appear that the calculation of radiant energy incident on an element of tube surface can be carried out by assuming

that the fin and the opposite tube are longitudinally isothermal and of infinite length. This is, in fact, the quasi-two-dimensional treatment employed in reference 4.

CONCLUDING REMARKS

The investigation reported herein has considered two effects that have generally been neglected in prior studies of fin-tube radiators: (1) the longitudinal conduction of heat in the fin and (2) the effect of longitudinal temperature variation and finite radiator length on the radiant interchange between radiator elements. It has been shown that longitudinal conduction is negligible for practical values of the governing parameters appropriate to space-vehicle power systems. It has also been demonstrated that the radiant interchange can be calculated with sufficient accuracy by assuming longitudinally isothermal surfaces that are essentially infinite in length.

These conclusions indicate that the problem can be treated in a quasi-two-dimensional manner, as in reference 4. The results of reference 4 can be generalized to a situation with longitudinally varying temperature by a step-by-step method of the type described herein.

Heat Transfer Laboratory
Department of Mechanical Engineering
University of Minnesota
Minneapolis, Minn.
July 30, 1963

REFERENCES

1. Lieblein, Seymour: Analysis of Temperature Distribution and Radiant Heat Transfer Along a Rectangular Fin of Constant Thickness. NASA TN D-196, 1959.

2. Bartas, J. G., and Sellars, W. H.: Radiation Fin Effectiveness. Jour. Heat Transfer (Trans. ASME), ser. C, vol. 82, no. 1, Feb. 1960, pp. 73-75.

3. Sparrow, E. M., Eckert, R. G., and Irvine, T. F., Jr.: The Effectiveness of Radiating Fins with Mutual Irradiation. Jour. Aerospace Sci., vol. 28, no. 10, Oct. 1961, pp. 763-772, 778.

4. Sparrow, E. M., and Eckert, E. R. G.: Radiant Interaction Between Fin and Base Surfaces. Jour. Heat Transfer (Trans. ASME), ser. C, vol. 84, no. 1, Feb. 1962, pp. 12-18.

5. Sparrow, E. M., and Jonsson, V. K.: Angle Factors for Radiant Interchange Between Parallel-Oriented Tubes. (To be pub. in Jour. Heat Transfer.)

TABLE I. - DIMENSIONLESS FIN-BASE TEMPERATURES $\Theta_b(Z)$ AT Z, $N_{ci} = 1$

(a) $N_b = 0.4$

Dimensionless coordinate, Z	Solution of eq. (11)	Step-by-step method
0	1.0	1.0
1/6	.9662	.9662
2/6	.9356	.9356
3/6	.9077	.9077
4/6	.8823	.8822
5/6	.8589	.8588
1	.8373	.8372

(b) $N_b = 0.7$

Dimensionless coordinate, Z	Solution of eq. (11)	Step-by-step method
0	1.0	1.0
1/6	.9428	.9429
2/6	.8945	.8946
3/6	.8530	.8531
4/6	.8170	.8171
5/6	.7854	.7855
1	.7574	.7575

TABLE II. - TEMPERATURE DERIVATIVES FOR THE ONE-DIMENSIONAL CONDUCTION EQUATION (3)

Fin-conductance parameter, N_c	Temperature derivative, $\left[d(T/T_b)/dX\right]_{X=0}$
1.00	-0.5323
.95	-.5149
.90	-.4972
.85	-.4788
.80	-.4598
.75	-.4403
.70	-.4200
.65	-.3991
.60	-.3774
.55	-.3549
.50	-.3314
.45	-.3068
.40	-.2811

TABLE III. - LONGITUDINAL VARIATION OF FIN-TO-TUBE ANGLE FACTOR[a]

Longitudinal distance, $\Delta Z = \lvert Z_t - Z \rvert$	Angle-factor ratio, $\left[dF_{dA_f - dA_t}\right] \Big/ \left[dF_{dA_f - dA_t}\right]_{\Delta Z=0}$
0	1.0
.05	.0155
.10	.00232
.15	.00060
.20	.00021
.25	.000091
.30	.000045

[a]The symbol dA_t is used as an abbreviation for $(dA_1 + dA_2)$.

TABLE IV. - ENERGY INCIDENT ON FIN SURFACE ELEMENTS

Dimensionless coordinate, X	Incident-energy ratio, $e_i(X)/e_i(0)$	
	e_i obtained from eq. (13)	e_i obtained from eq. (15)
Dimensionless coordinate, Z, 0.06		
0	1.0	1.0
.1	.408	.410
.2	.266	.268
.3	.193	.195
.4	.150	.152
.5	.122	.125
.6	.104	.107
.7	.0924	.0952
.8	.0848	.0877
.9	.0805	.0836
1.0	.0792	.0822
Dimensionless coordinate, Z, 0.5		
0	1.0	1.0
.1	.410	.410
.2	.268	.268
.3	.195	.195
.4	.152	.152
.5	.125	.125
.6	.107	.107
.7	.0954	.0952
.8	.0880	.0877
.9	.0838	.0836
1.0	.0825	.0822
Dimensionless coordinate, Z, 0.94		
0	1.0	1.0
.1	.409	.410
.2	.267	.268
.3	.194	.195
.4	.151	.152
.5	.124	.125
.6	.106	.107
.7	.0940	.0952
.8	.0865	.0877
.9	.0823	.0835
1.0	.0809	.0822

TABLE V. - LONGITUDINAL VARIATION OF TUBE-TO-TUBE ANGLE FACTOR

Longitudinal distance, $\Delta Z = \lvert Z_{t,2} - Z_{t,1} \rvert$	Angle-factor ratio, $\left[dF_{dA_2-dA_1} \right] \Big/ \left[dF_{dA_2-dA_1} \right]_{\Delta Z=0}$
0	1.0
.05	.452
.10	.116
.15	.0350
.20	.0132
.25	.0059
.30	.0030

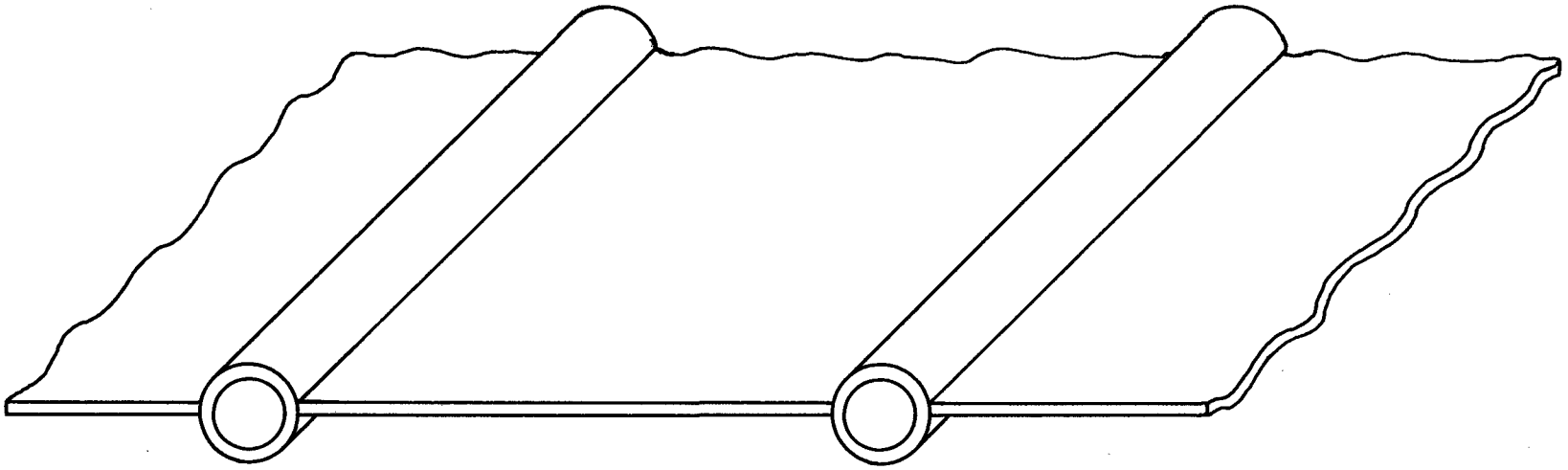

Figure 1. - Schematic of fin-tube radiator with central fin.

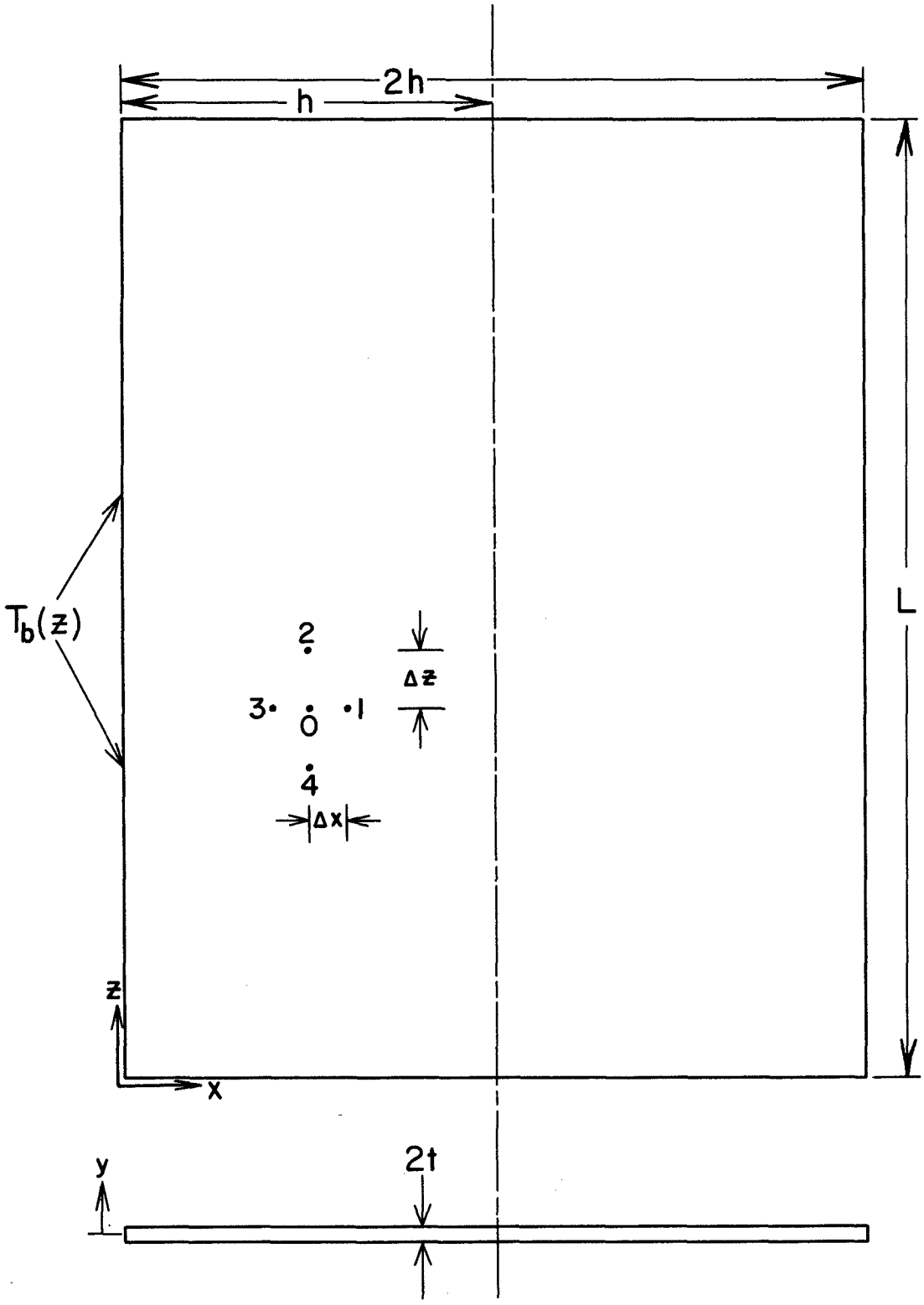

Figure 2. - Coordinates and nomenclature for analysis of longitudinal conduction in radiator fin.

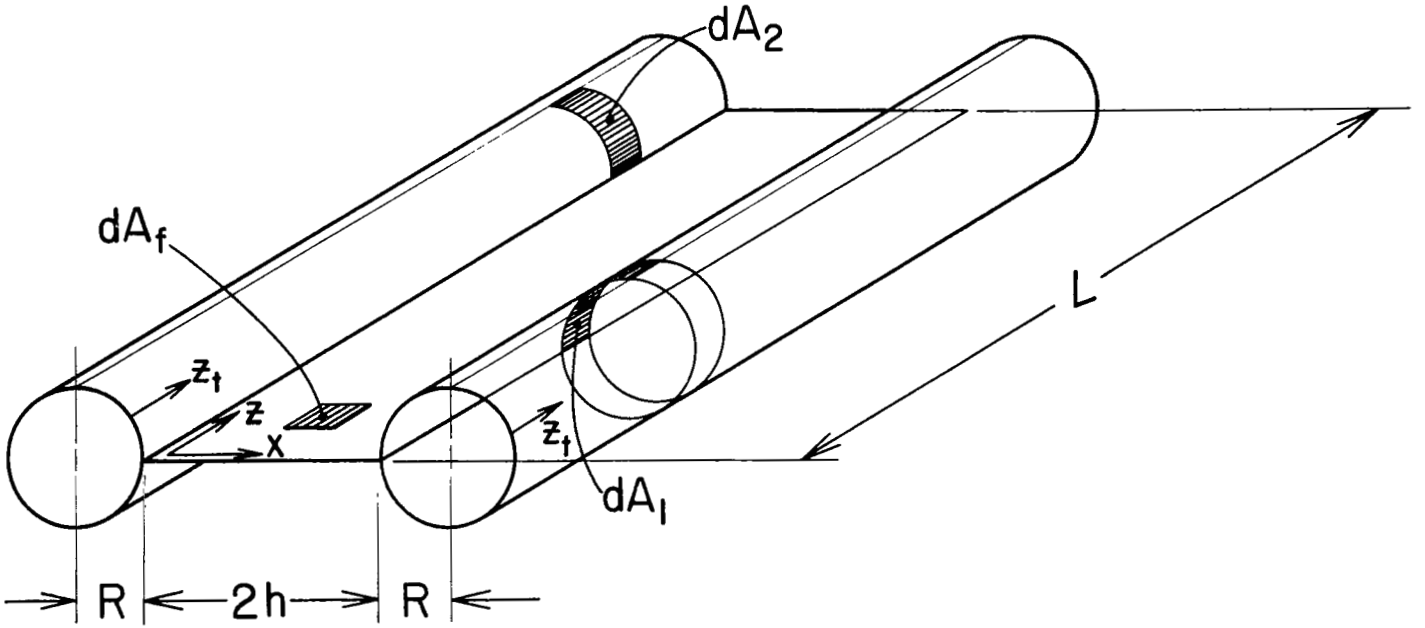

Figure 3. - Coordinates and nomenclature for analysis of radiant interchange.